Keynote lecture presented at Geotechnical Challenges in Urban Regeneration, the 11th International Conference of the DFI-EFFC, London, 26-28 May 2010.

PREDICTING AND CONTROLLING GROUND MOVEMENTS AROUND DEEP EXCAVATIONS

Malcolm D. Bolton, Sze Yue Lam and Paul J. Vardanega

ABSTRACT

Deep excavations frequently cause problems, and sometimes trigger catastrophic collapses, especially in soft clay. In principle, these problems are well understood, but designers may fall between the two stools of naive empiricism and over-elaborate finite element analysis (FEA). A new approach, Mobilizable Strength Design (MSD), has been developed to bridge this gap. MSD specifies deformation mechanisms tailored to each stage of construction. Each stage is analysed for energy balance, with incremental subsidence creating a drop of potential energy which must equal the work done deforming the soil and the support system. Incremental deformations are summed, while soil non-linearity is allowed for. The non-linear response of a representative shear stress-strain test is required, but estimates can be based on routine soil characterisation. It is demonstrated that MSD back-analyses not only fit FEA results for soft clay within ± 30%, but also fit the soil-structure deformation data of 110 field studies within a factor of 1.4. Finally, a new set of dimensionless groups is defined to characterise deep excavations in clay without the need for any analysis at all. These are used to chart the maximum wall displacements taken from the field database, and an elementary formula is proposed which predicts these 110 maximum displacements within a factor of 2.9. Guidelines are deduced for designers. In particular, it is shown that wall stiffness within the typical range of sheet-piles, secant piles and diaphragm walls has little or no effect on wall deformations.

MOTIVATION

Urban regeneration calls, above all, for rapid transit links. The *raison d'etre* of a city is the capacity of its citizens to perform transactions in person. This calls for travel: to work and play, to buy and sell goods, to offer and access services. However, the recent rate of growth in car travel is unsustainable. In order to reduce carbon dioxide emissions, other pollutants, and noise, car travel must be replaced by mass rapid transit systems. Cities around the world are attempting to regenerate or expand by building subways. At the same time, property developers are specifying deep basements which maximise land use. All these trends call for deep excavations.

THE STATE OF THE ART

Structures

Excavations can be made by driving deep soldier piles supporting lateral boards or sheets which retain the earth. Interlocked steel sheet-piles have generally superseded them in the absence of buried obstacles. However, such flexible retaining systems may bend and bulge excessively when the depth of excavation begins to mobilise a significant fraction of the soil's available strength. Props at regular vertical intervals can be used to brace parallel sides apart, sacrificing some mobility and workspace inside the excavation. But for deeper excavations in soft ground the incremental displacements, which accrue with every stage of excavation before a new level of props can be placed, can give rise to significant bending moments in the walls and to subsidence affecting neighbouring structures and services.

It is believed that cast insitu reinforced concrete retaining walls offer some mitigation of these effects. Cement stabilization can alternatively be used to create gravity walls. Wherever possible, the bases of walls are fixed within hard layers underlying the soft ground. As excavation proceeds, props or anchors are installed to prevent excessive inward movement of the walls.

Speed of construction is often an issue, and it has become popular to design the excavation support system as part of the permanent structure, rather than as temporary works. A ground floor slab can be cast as a prop at the crest of the retaining walls so that the superstructure construction can proceed above, at the same time as "top-down" excavation beneath the ground floor slab permits the successive casting of basement slabs which also act as props.

In very deep soft soils it may not be possible to fix the bases of the walls in stiff ground. It may then be necessary to use jet-grouting or deep soil mixing, for example, to introduce a cemented plug between the bases of the walls prior to excavation. Such a plug can serve two functions: as a compression plug acting as a prop, and as a shear plug preventing base heave.

Soil mechanics

The classical soil mechanics literature of earth retention is expressed in terms of the fully active and fully passive earth pressures, σ_a and σ_p. Expressions are developed in terms of Mohr-Coulomb strength envelopes, described either by the undrained shear strength c_u, or the drained shear strength ϕ'. For example, in Rankine's simple analysis for frictionless walls retaining level ground with a hydrostatic water table:

$$\sigma_a^p = \gamma z \pm 2c_u \qquad (1)$$

$$\sigma_a^p = \gamma_w z_w + (\gamma z - \gamma_w z_w)\tan^2(45 \pm \phi'/2) \qquad (2)$$

where z is the depth below ground level, z_w is the depth below the water table, and γ and γ_w are the unit weights of the bulk soil and of the water, respectively, and ± refers to passive (+) and active (–) pressures for peak soil strengths. Plasticity theory permits the creation of formulae or tables which extend these elementary results to rough, sloping walls retaining sloping ground. Coulomb's wedge analysis can easily be programmed to compute more complex stratifications and groundwater variations, but it must be recalled that assumed mechanisms always provide solutions somewhat on the unsafe side.

Base heave can similarly be treated with simple strength parameters in ideal cases. The undrained shear failure of soft soil can be treated as a negative bearing capacity failure, with a factor N_c in the range 5 to 8 as a function of excavation geometry:

$$\gamma H_{\max} = N_c c_u \qquad (3)$$

Base heave in the fully drained case will occur when the passive thrust exerted by the retaining walls overcomes the vertical effective stresses beneath the excavation, which will be reduced by upward seepage.

Significant uncertainties arise in practical applications, of course. First, the designer must exercise judgement in order to choose a value of c_u or ϕ' whilst recognising spatial variability. Secondly, soil will often be partially drained. An analyst might suggest using a Finite Element Analysis (FEA) coupling deformation and transient flow to compute an earth pressure that would presumably change from an undrained to a drained value. However, the uncertainty and variability in ground permeability is even greater than that for other soil characteristics.

Finally, and most significantly, the strains that can be tolerated around a deep excavation will generally be much smaller than those required to mobilise peak soil strength, making parameters c_u and ϕ' inapplicable. The response in practice is generally to rely on "factors of safety" specified in Codes of Practice, Guides and Regulations. A more analytical response would be to run an FEA with appropriate soil deformation parameters. But this requires exceptionally good judgement in the selection of mathematical models for soil behaviour, and in obtaining representative values of the defining parameters.

At issue is the difficulty that practising engineers habitually measure the strength of soil, not its stiffness. It is even common for designers to eschew proper stress-strain testing altogether in favour of probing with SPTs, for example. This cavalier approach to material testing fits very badly with the trend amongst academic research workers over the last 30 years to develop ever more sophisticated constitutive models. These will usually have been validated against equally sophisticated batteries of triaxial tests on initially identical samples of archetypal soils reconstituted and reconsolidated in the laboratory. But for real, variable, soils it will be impossible to fix values for the 20 or 30 parameters that complex constitutive models usually possess.

The practising engineer who wishes to deal explicitly with ground strains is currently left performing FEA with simpler soil models. Since soil is quite non-linear, the use of linear-elastic perfectly-plastic soil models is beset by the problem of selecting an appropriate secant stiffness through a curve. It would therefore appear best to attempt to define the stress-strain curves of representative samples of soil, and to use these curves directly in FEA. This approach was first outlined by Duncan and Chang (1970) who fitted a hyperbola between an initial elastic stiffness and a peak plastic strength. Reasonable correspondence has been reported between measured excavation performance and FEA back-analyses based on sampling, testing and the judicious fitting of hyperbolae. Nevertheless, designers are left acutely conscious that the risk of error in terms of ground deformations is currently unquantifiable.

Groundwater flow

The designer must also consider the consequences of groundwater pressures giving rise to flow. Water tends to flow into deep holes, through the walls and beneath the excavation. If it is decided to keep the excavation dry, a sump within the excavation may be sufficient in fine-grained soils. But in every case it is necessary to consider the base heave which may be caused by deep water pressures. A catastrophic heave failure will occur when a deep, permeable soil layer beneath the excavation can maintain a water pressure as high as the self weight per unit area of the overlying soil that remains. This is a particular danger in soil profiles with clay overlying sand because the contrast in permeability can maintain high water pressures in the sand as the clay is excavated. For excavations in coarse grained soils the heave failure criterion is equivalent to there being a critical upward hydraulic gradient which can eliminate all effective stress beneath the excavation, leading to liquefaction or piping with internal erosion.

Even if the deep water pressures are smaller than those required for gross heave, they can create sufficient softening to severely reduce passive pressures below the excavation if the soil has time to swell in response to the removal of overburden. These threats may lead the engineer to provide for deep dewatering. However, any removal of groundwater from the vicinity of an excavation will tend to lower the external water pressures leading to subsidence which can affect a wide area. Local subsidence can be caused by sand production from badly screened wells or water ejectors.

An alternative solution to dewatering may be to prop the walls apart at the crest, then flood the excavation as it is made, ultimately casting a concrete base slab under water: Clarke and Prebaharan (1987). If the inevitable construction difficulties can be overcome, the soil support system will be complemented by water pressures, and no transient flow need occur.

RISK

The creation of subways appears to be a particularly risky business both for the construction team involved and for the neighbours. Deep excavations for cut and cover tunnels, station boxes, and shafts are the subject of this paper. In the last six years alone there have been several catastrophic collapses, each with multiple deaths and injuries, and each posing a severe commercial threat to the companies involved in design and construction and a political embarrassment for the promoters.

These collapses include:

- the braced diaphragm wall excavation for approach tunnels to the Nicoll Highway subway station in Singapore in March 2004,
- the 40m diameter sprayed concrete shaft construction at Pinheiros Station in Sao Paolo in January 2007,
- the access tunnel to Suzhoujie Station under construction in Beijing in March 2007,
- the braced excavation for the Xianghu subway station construction in Hangzhou in November 2008,
- the Cologne city archives building falling into the anchored diaphragm wall excavation for the construction of Severinstrasse subway station in March 2009,
- and the braced excavation for Sajinqiao subway station in Xi'an in August 2009.

When such serious incidents occur, the emergence of an engineering account of the probable causes is often hampered by the commercial, legal and political processes which generally take precedence. An exception is the Singapore Government's Committee of Inquiry (Magnus et al, 2005) into the Nicoll Highway collapse, which facilitated a review by international engineering experts, ultimately providing public access to the findings of serious design flaws. Of these, two were found to be paramount:

- an erroneous characterisation of the soft Singapore marine clay in computer software, which led to an overestimation of its undrained strength by a factor of about 2 and thereby to an underestimation of the wall bending moments and the strut forces, albeit by a much smaller margin;
- an under-design of the steel connections between struts and waler beams, which failed unstably by buckling at about half their intended capacity.

The COI put these particular failings into a much broader context, calling for clearer designation of responsibilities and a reflective approach to the identification of hazards and the management of risks. For example, the COI drew attention to the large wall deformations (in excess of 400mm) that had been observed to occur prior to collapse, and to the potential for monitoring to reveal incorrect design assumptions long before ultimate catastrophe. The Singapore Government Building and Construction Authority (BCA) took immediate steps in their Advisory Note 1/05 to bring deep excavations into a clear regulatory framework, notwithstanding their having previously been classed as "temporary works". This has itself prompted some vigorous discussion within the profession, and thereby to amendments in the

recommended procedures which were embodied in BCA Advisory Note 1/09. Whatever one's views of the merits of Government regulation, the professionalism and transparency of the Singaporean approach should be commended.

In three of the other catastrophic collapses listed above, press reports speculated that the potential significance of ground movements may have been overlooked as construction continued. And the availability of water – from rain storms, broken pipes, or a nearby river – was often linked with the sequence of events on the day in question. Of course, ground movements can lead to water release, as well as the other way round. Significant ground movements can cause joints to open up in fresh or foul water services, and resultant erosion and cracking can lead to the unexpected arrival of water in the vicinity of the excavation. Such water may have two deleterious effects on the stability of earth retaining structures, an increase of active forces due to the full-height hydraulic thrust acting on the retained face, and the removal of passive support due to upward seepage in the excavation which could even lead to soil liquefaction, piping or base heave.

In the absence of further information in these other cases, one can only presume that some combination of the following shortcomings was responsible for the catastrophe:

- the actual ground profile (such as the depth of soft layers, their strength, etc) was less favourable than that assumed in design;
- the groundwater regime was less favourable than that assumed in design;
- the surcharge loads actually applied to the retained surface exceeded those that had been allowed for;
- the sequence of excavation stages in relation to the placement and pre-loading (if any) of supports, was more aggressive than had been allowed for;
- the behaviour of one or more of the structural components of the wall and its supports, whether props or anchors, was inferior to what had been assumed in design;
- the composite system behaviour of the ground and the support structure differed from that assumed in design, to such an extent that excessive deformations and displacements were induced during excavation.

The first five require robust integration between design, ground investigation and inspection procedures during construction. It is the sixth, the creation of a strain-based theory of soil-structure interaction, which this paper addresses, enabling a link to be made between "factor of safety", wall deformation, and ground movement.

THE OPPORTUNITY FOR IMPROVEMENT

In their General Report on Deep Excavations, Tan and Shirlaw (2000) remark that in view of the uncertainties in ground conditions, analytical methods, and construction procedures, engineers generally follow "...a wise course; they build a sufficiently stiff retaining and bracing structure which is so strong that the stiffness of soil contributes little to the overall stiffness of the soil structure system." If so, these engineers are treating the soil rather like a heavy fluid into which a support structure has to be introduced to maintain a reduced "fluid" level corresponding to the excavation, with lateral bracing carrying lateral earth pressures, and with some means of preventing the "fluid" entering from below.

One might therefore compare the construction of a deep excavation in soft soil with the construction of a ship "top-down", floating in heavy water. Of course, a marine architect has the advantage of designing a ship to be built bottom-up, from the keel, on dry land. So the half-built vessel will be subject only to gravity while it is being constructed, not to external soil or water pressures, and formwork can be used to prevent deformation. The final geometry of the ship can be predicted and controlled within tight tolerances, so the design can incorporate single or double hulls with prefabricated beams, plate stiffeners and stanchions – all welded in place to create an efficient integral structure. Clear load paths, following lines of relative stiffness, enable a straightforward set of design rules to be used to produce an initial design that should be safe and serviceable in the specified loading scenarios of waves and cargo. The initial design can later be finessed by finite element analysis to reduce weight and enhance fatigue resistance, for example.

The promoters of underground constructions must regret that their schemes proceed with an order of magnitude less predictability than the building of a boat. But they might admire the ingenuity of the *in situ* construction process in the light of comparative costs. A medium-sized oil tanker might offer useful cargo space of 80 000 m^3 for a construction cost of about £1200 per m^3. The Westminster underground station box for the Jubilee Line Extension created a similar underground volume and was tendered at about £1000 per m^3 at today's prices, but the complexities of the site and the need to protect the adjacent Big Ben clock tower added very considerably to the final construction cost.

Is further economy possible? In his General Report, six years after Tan and Shirlaw, Boone

(2006) reflected on whether a less conservative approach to deep excavation design could be advocated. In view of the risks and uncertainties he concluded: "Presently, no.". But he did make "the following proposal...

- if sufficient testing can be carried out or collected for specific soil deposits, the uncertainty (variability) of the engineering properties may be characterised;
- if a sufficient number of Class A predictions can be made and compared to field measurements, the uncertainty in analysis methods may be defined;
- if a sufficient number of case histories can be collected with appropriate identification of construction details, the uncertainty related to workmanship and process details may be characterised;

then it may be possible to complete reasonable stochastic analyses of excavations so that the probability of achieving performance goals could be quantitatively evaluated, designs optimized, cost-effectiveness improved, and better decisions made." Boone called for focussed research to that end.

This paper reports work at Cambridge University that has been devoted to this challenge. Responses are given in each of the three areas of challenge – a database of soft clay stiffness, the creation and validation of a new theory, and the performance of that theory in back-analysing a new database of excavation case histories.

USING A DATABASE OF SOIL STIFFNESS

Geotechnical engineers have traditionally approached serviceability and deformation issues through elastic-style calculations based on some stiffness modulus. Soil is linear elastic at very small strains (e.g. shear modulus G_{max} at shear strain $\gamma < 10^{-5}$), but it then suffers a progressive deterioration of secant stiffness $G = \tau/\gamma$, up to its peak strength c_u. This non-linearity is generally expressed through the normalisation $G/G_{max} = f(\gamma)$. However, it will be useful here to characterise the mobilised shear stress $\tau = c_{mob}$ ($< c_u$) $= G\gamma = f^*(\gamma)$. We can then deduce the shear strain γ that would be experienced at some mobilised shear stress c_{mob} smaller than the peak undrained shear strength c_u.

This mobilisation of strength approach has been used by Vardanega and Bolton (2010) to present the data of 13 soft clays and silts previously published by Anderson and Richart (1976), Kim and Novak (1981) and Shibuya and Mitachi (1994). For this purpose, normalisation of both stress and strain axes is required. Shear stress, or mobilised strength, is presented as a proportion of the peak undrained shear strength, c_{mob}/c_u. Shear strain is normalised in relation to a reference strain corresponding to the mobilisation of peak strength, γ/γ_u. The reference strain γ_u should be derived by extrapolating a best-fit parabola through the central segment of stress-strain data ($0.2 < c_{mob}/c_u < 0.8$) until it reaches peak strength. Each such parabola is constrained to have its apex at the origin. The excellent outcome for the 13 soft clays is shown in Figure 1. It is also evident that a linear lower bound may be advised at small mobilisations, $c_{mob}/c_u < 0.2$.

BS8002 (1994) defines c_u/c_{mob} as the mobilisation factor M which is equivalent to a "factor of safety" on shear strength, though it was explicitly concerned with limiting deformations rather than with safety as such. Accordingly, the mobilisation of shear strength in soft to firm clays (OCR < 5) can simply and accurately ($R^2 = 0.98$) be written:

$$\gamma/\gamma_u = 0.2\, c_{mob}/c_u = 0.2 / M \qquad \text{for } M > 5 \qquad (4a)$$

$$\gamma/\gamma_u = (c_{mob}/c_u)^2 = 1 / M^2 \qquad \text{for } M < 5 \qquad (4b)$$

It remains necessary, of course, to select appropriate values for c_u and γ_u in any given case, ideally through tests on high-quality cores, or through self-boring pressuremeter tests. However, a statistical correlation between γ_u and plasticity index I_p, obtained by Vardanega and Bolton (2010), and shown in Figure 2:

$$\gamma_u = 0.024(I_p)^2 + 0.0031 \qquad (R^2 = 0.81) \qquad (5)$$

permits the engineer to select a reasonable value for lightly overconsolidated clays and silts.

In applying equations 4 and 5 it should be noted that they were derived using the data of cyclic tests. It was implicitly assumed that strain rate would have effected c_{mob} and c_u values equally, and would have cancelled out. Ideally, an engineer should perform a stress-strain test on a representative sample at a strain rate appropriate to the design situation. However, the errors incurred by applying a simple rule such as 5% strength enhancement on c_u per factor ten increase in strain rate, following Vucetic and Tabata (2003), might be considered acceptable. Equation 4 could then be applied with a rate-corrected strength c_u^* and the reference strain γ_u obtained from equation 5 in order to estimate soil strains in service. In some circumstances, a designer might even be prepared to infer c_u from an SPT blowcount, following Stroud (1974), in order to make a preliminary assessment of ground strains using (4) and (5).

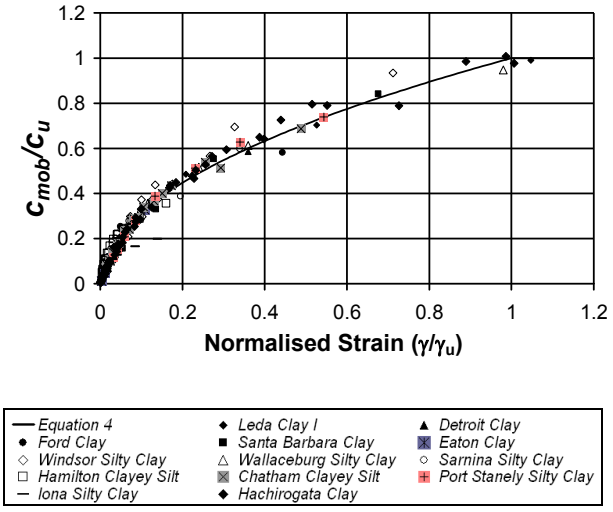

Figure 1 Normalisation of shear stress-strain curves from cyclic torsional tests on clays

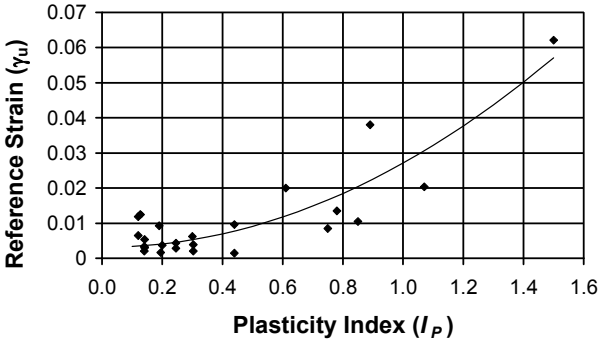

Figure 2 Dependence of reference strain γ_u on soil plasticity index I_p

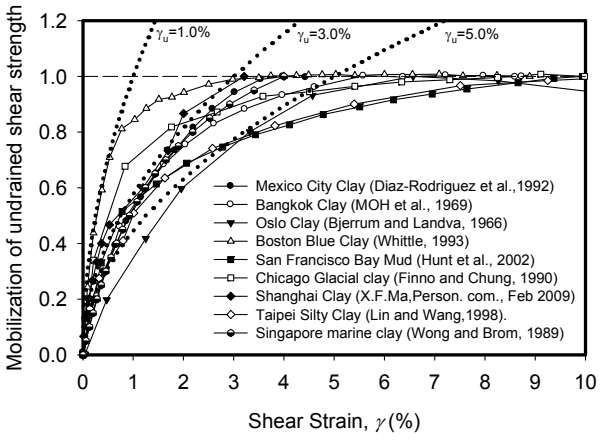

Figure 3 Mobilisation curves for various case histories of deep excavation

However, a point of caution should be noted regarding the simplified parabolic-to-peak mobilisation curve of Figure 1. Monotonic triaxial tests on "undisturbed" samples of soft clay are sometimes found to give strains in excess of the parabolic fitting for $c_{mob}/c_u > 0.8$. See Figure 3, taken from Lam and Bolton (2010), for examples of shear stress-strain mobilisation curves associated with field records of deep excavations in soft clay, for example. Furthermore, most normally consolidated clays are sensitive, so their available strength reduces with increasing strain after the peak. It would therefore be prudent not to permit a mobilisation factor $M < 1.2$ for design purposes unless the retaining wall is fixed in a hard layer at its base, and is sufficiently stiff to control soil strains.

Finally, it is necessary to review what has been omitted from this section. Firstly, overconsolidated clays may be found to have a smaller reference strain γ_u than the same clay when it is normally consolidated. Secondly, the strength mobilisation of granular soils has not been addressed here. And thirdly, no mention has been made of the volume changes which may follow or accompany shear. Work is in hand in Cambridge on each of these aspects with a view to deriving simple design rules for the limitation of soil strains in these cases also.

GROUND DEFORMATION MECHANISMS

Figure 4 shows various simplified deformation mechanisms applicable to retaining structures supported in different ways. In each case, deformations in the shaded zone are ignored in favour of a specified zone of finite shear strains giving rise to ground and wall deformations that are consistent with the boundary conditions.

These mechanisms require that the soil deforms at constant volume – "undrained" in the context of clays deforming during excavation. They can be used to produce approximate solutions for ground deformations in a fashion analogous to the use of slip circles or wedges in collapse limit analysis. And, in the spirit of upper bound limit analyses, they tend to overestimate the depth of excavation that will generate a given volume of subsidence. Just as with limiting equilibrium solutions, these "limiting deformation" solutions therefore need to be checked against FEA, centrifuge models, or field records to ensure they are adequate.

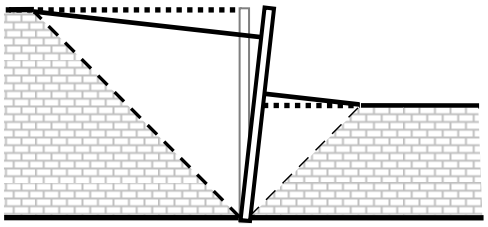

a) stiff wall pinned at its base in a hard layer

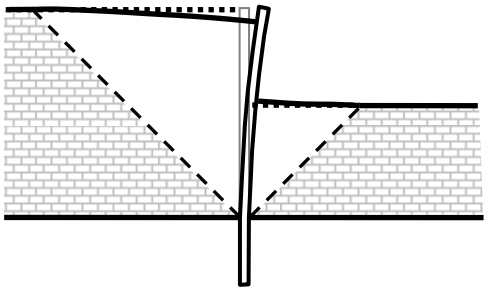

b) flexible wall fixed at its base in a hard layer

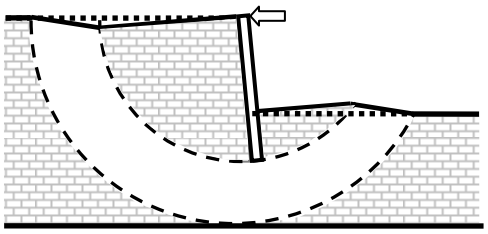

c) stiff wall propped at its top

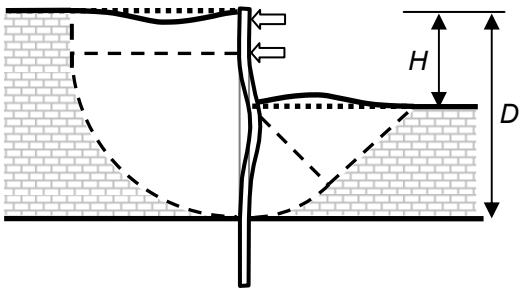

d) flexible wall bulging below fixed props

Figure 4 Simplified deformation mechanisms

MOBILIZABLE STRENGTH DESIGN (MSD)

The first application of MSD was to rigid, smooth, cantilever retaining walls in clay: Bolton and Powrie (1988). The wall was supposed to respond to excavation by rotating about a point just above its toe, creating active and passive zones either side, but restricting the strength in equation 1 to a value $c_{mob} < c_u$. The equations of lateral and moment equilibrium were written down and solved for c_{mob}. The mobilised shear strain γ could then be read off a representative stress-strain curve, and the wall rotation θ could be deduced from the relation $\gamma = 2\theta$, derived from Mohr's circle of strain. Centrifuge model tests showed that this approach can provide reasonable accuracy, notwithstanding the simplifications of focusing only on near-field soil deformations (see Figure 4a) and ignoring the influence of wall roughness.

A follow-up study by Osman and Bolton (2004) compared MSD based on wall rotation with FEA for "floating" cantilever walls, and showed that the influence of $K_o \neq 1$ could be accounted for if the data of compression and extension tests were separately available. Neither wall friction nor the precise shape of a soil's stress strain curve caused MSD calculations to depart excessively from FEA computations. However, one factor not included in the MSD wall rotation model was significant in the FEA: the base of the wall translated towards the excavation. Effectively, FEA showed that a "floating" wall analysis invoking only wall rotation (Figure 4a) caused MSD to underestimate wall crest displacements by up to a factor of 2. MSD needs to include wall bending (Figure 4b), and deep foundation shearing (Figure 4c), if more precise predictions are to be made.

These aspects were considered by Osman and Bolton (2005) in the application of MSD to braced excavations, which specifically addressed the bulging that is seen below the bottom row of props when the excavation is advanced. Each increment of bulging can be predicted reasonably well by assuming the bulge to be sinusoidal, following O'Rourke (1993). Figure 4d shows a wall fixed in a hard layer, for which the wavelength of the bulge at any stage of excavation equals the distance between the bottom row of props and the bottom of the soft clay. Where there is no hard layer, virtual fixity can be imagined at a depth below the wall base equal to half the unsupported wall length below the bottom prop. Wall displacement calculations begin with the cantilever stage (Figure 4a) as an excavation is made for the top level of props. Progressive displacements are found by superposing each stage of wall bulging (Figure 4d) as excavation proceeds below the most recently fixed row of struts. Calculated wall displacements fell within ± 30% of field records.

These predictions of flexural deformation required a different calculation method based on the conservation of energy within the deformation mechanism, as set out by Bolton et al (2008). The loss of potential energy, represented by the formation of a subsidence trough in the retained ground while the soil within the excavation heaves, must be balanced by the work done deforming both the soil and the retaining structure.

The loss of potential energy during any given stage of excavation is quite easily calculated as:

$$\Delta P = \Sigma\, (\rho g\, \Delta z)\, \delta A \qquad (6)$$

where the weight $\rho g\, \delta A$ of each element of soil of area δA within the mechanism is associated with its average settlement Δz. Each settlement Δz must be deduced from the sinusoidal displacement profile "flowing" through the mechanism in that stage.

The work done on the soil is calculated using the swept area under the soil's stress-strain curve. For example, Figure 5a demonstrates that the work done per unit area in straining soil by amount γ along a parabola (equation 4a) is:

$$\delta W_{soil} = \frac{2}{3}\tau\gamma = \frac{2}{3}c_u\left(\frac{\gamma}{\gamma_u}\right)^{0.5}\gamma = \frac{2}{3}\frac{c_u}{\gamma_u^{0.5}}\gamma^{1.5} \qquad (7)$$

The magnitude of strain γ has to be calculated from the sinusoidal displacement field. Then the total work done on the soil, starting from an undeformed state, is found by integration over the whole area of the mechanism:

$$\Delta W_{soil} = \sum \delta W_{soil}\, \delta A \qquad (8)$$

The work done in bending the wall from its initially undeformed state is calculated from the area under the moment-curvature relation. Figure 5b shows that for a wall segment of unit length with a flexural stiffness EI developing a curvature κ:

$$\delta W_{wall} = \frac{1}{2}M\kappa = \frac{1}{2}EI\kappa^2 \qquad (9)$$

The magnitude of curvature has to be calculated from the second differential of the sinusoidal wall deflections. Then the total flexural work done on the wall is found by integrating over the length of the wall:

$$\Delta W_{wall} = \int \delta W_{wall}\, dx \qquad (10)$$

The fundamental energy conservation equation of MSD is then, simply:

$$\Delta P = \Delta W_{soil} + \Delta W_{wall} \qquad (11)$$

This can be solved iteratively for each stage of excavation, using the maximum wall displacement Δw_{max} in that stage as the unknown. The subsidence increment is the same. Finally, these increments can be superposed to obtain the overall maximum displacement w_{max}.

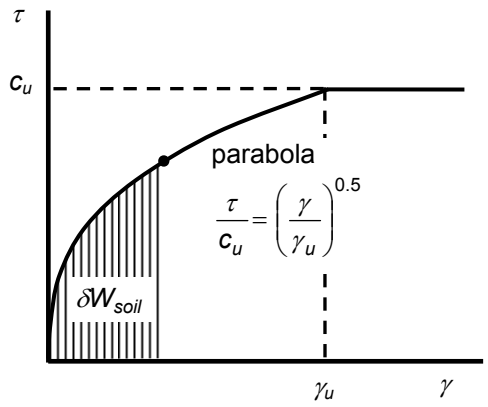

a) Work done per unit volume of soil

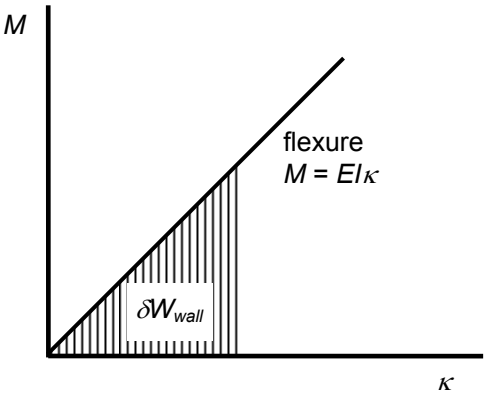

b) Work done per unit length of wall

Figure 5 Unit work calculations

Bolton et al (2008) took care to recognise the incremental and non-linear nature of this energy balance in the calculations they advanced. It is necessary to store the previous shear strain of each element of soil so that the work done due to the next increment of excavation can properly be calculated with respect to the non-linear stress-strain curve. A similar sort of procedure has to be used for the structural strain energy since this is also non-linear, having a quadratic relation to wall displacement and curvature.

Other important details were addressed, including the need to use a different mechanism when the excavation is narrow compared with its depth, and ensuring that the ground model could incorporate layers with different soil properties. In this fashion, they set out to compare MSD predictions of braced excavation performance with those of FEA conducted by Jen (1998) for a "floating" wall, with the parameters recorded in Figure 6. Typical bulging wall profiles from Bolton et al (2008) are compared in Figure 7 for a 17.5 m deep excavation supported at 2.5 m intervals, against a 40 m deep wall in a 100 m deep profile modelled as Boston Blue Clay. Excavation width B is varied from 30 m to 60 m.

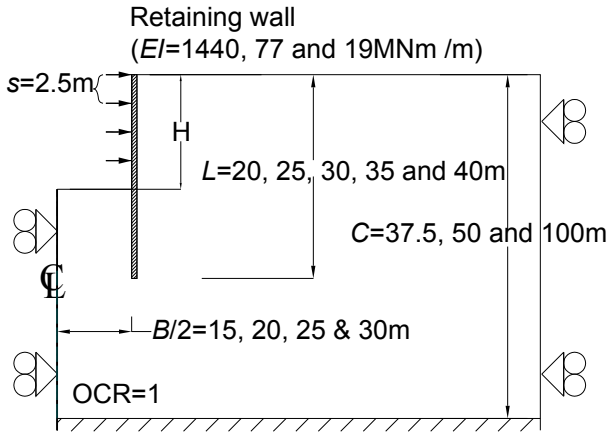

Figure 6 FEA carried out by Jen (1998)

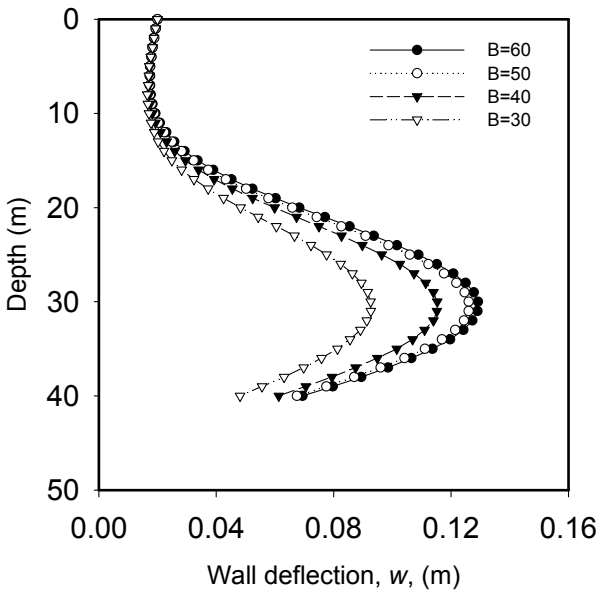

(a) Prediction by MSD

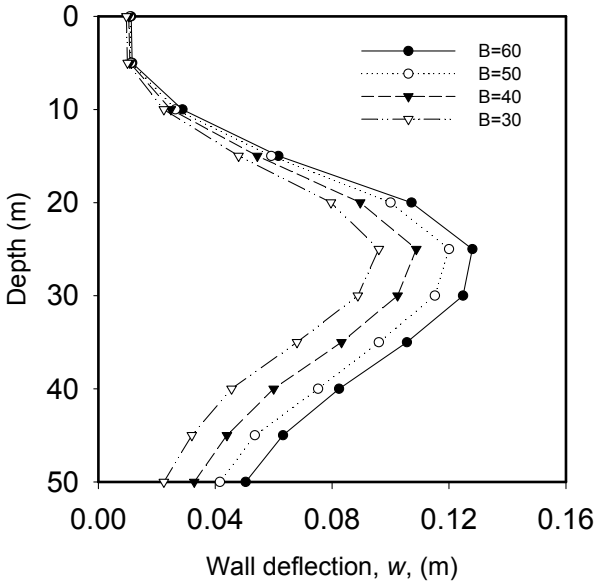

(b) Prediction by MIT E3 model (After Jen,1998)

Figure 7 Wall deflections for various widths B

Although MSD, working in a matter of minutes on a spreadsheet, does not precisely accord with Jen's FEA, the correspondence is close enough for decision-making purposes. The two pre-requisites for success are to have a compendium of simplified deformation mechanisms for compatible soil-structure interaction which are sufficiently close to reality (or to a good computer-generated simulation of reality), and to be able to characterise the ground in relation to its density, strength profile and stress-strain relation. If these aspects are well-represented the MSD analysis can hardly go wrong, because the principle of conservation of energy can hardly be faulted.

A NEW DATABASE OF EXCAVATIONS IN SOFT CLAY

With the aim of gaining a better understanding of ground movements around deep excavations, a database of 155 case histories was collected from geotechnical journals, international conference proceedings, national technical reports, and dissertations. Studies from nine cities are included: Bangkok (2 sites), Boston (5), Chicago (10), Mexico City (1), Oslo (9), San Francisco (4), Shanghai (67), Singapore (21) and Taipei (36). Full details will be found in Lam (2010).

These cases focused on the deformation of braced walls supporting deep excavations in soft to firm clays (i.e. $c_u < 75$kPa). For each case history, information was extracted and analyzed regarding major factors such as soil properties, groundwater conditions, excavation geometry, stiffness of structural support system, construction method and soil type. A total of 110 out of these 155 case histories were so fully documented that an analysis could be conducted with the MSD method taking careful consideration of ground stratification, the undrained shear strength profile of the soft to firm clay, its stress-strain behaviour, and the elevation of the stiff base stratum within which deformations might be ignored.

Figure 3 showed the mobilization of shear strength versus strain in tests reported for the nine soils concerned. The case-specific information from the database was used directly in MSD to predict maximum wall displacements w_{max} for each stage of excavation, which are compared with authors' reported observations in Figure 8. Results show a correlation coefficient $R^2 = 0.91$ about the line 1:1. More than 90% of the MSD predictions fell within a factor of 1.4 of the corresponding observations. Considering the lack of any detailed account of soil anisotropy, the field performance of MSD may be considered quite satisfactory.

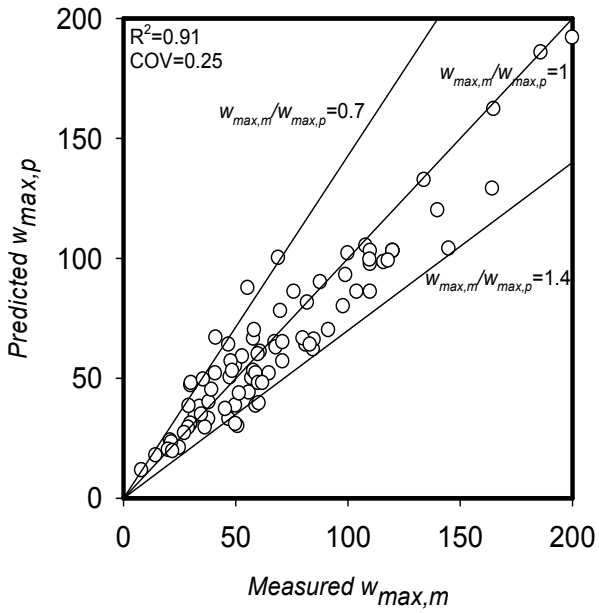

Figure 8 MSD calculations versus measurements

USING DIMENSIONLESS GROUPS

Whilst MSD can confidently be used to make site-specific predictions, it will also be helpful to use MSD concepts to derive dimensionless groups to chart data from field case studies, and to assist decision-making prior to any detailed analysis.

Consider first the normalization of maximum wall displacement w_{max} itself. MSD shows us, as in Figure 3, that the initial excavation to fix the top row of props generally produces relatively small movements at the crest in the cantilever phase of wall rotation or bending (Figure 4a,b). The most significant deformations for a fixed-base wall arise from later stages of construction when the wall bulges below the lowest props (Figure 4d). Elastic beam theory applied to the mechanism then teaches us that the change of net pressure necessary to produce a bulge of amplitude w_{max} over a wavelength λ will be

$$\Delta p \propto w_{\max} \frac{EI}{\lambda^4} \tag{12}$$

This can be normalised with respect to the reduction in vertical earth pressure ρgH due to excavation. Accordingly, a structural response ratio S can be defined:

$$S = \frac{w_{\max} EI}{\rho gH \lambda^4} \tag{13}$$

Whilst MSD permits λ to reduce progressively as props are placed deeper, a design chart might simply characterise the average situation, and an average λ value will be taken here as the distance between the middle props and the base of the deforming clay. We will define

$$\lambda_{average} = D - 0.5H \tag{14}$$

referring to Figure 4d, and we will use this value in equation 12.

Now consider the various system parameters that might modify the structural response ratio. It is proposed that they can best be visualised in combination as a soil-structure stiffness ratio R:

$$R = \frac{c_u}{\gamma_u} \frac{c_u}{\rho gH} \frac{\lambda^3}{EI} \tag{15}$$

where λ is again taken as the average value during the whole excavation process, and where the value of c_u is selected to represent the strength at mid-depth of the soft clay layer. The rationalisation is as follows. The ratio c_u/γ_u is the secant shear modulus just as peak strength is reached. For a parabolic shear stress-strain curve (equation 4b) we obtain the secant modulus mobilised at any earlier stage:

$$G = \frac{c_{mob}}{\gamma} = \frac{c_u}{\gamma} \left(\frac{\gamma}{\gamma_u} \right)^{0.5} = \frac{c_u}{\gamma_u} \left(\frac{\gamma_u}{\gamma} \right)^{0.5} \tag{16}$$

Using equation 4b again, we can write this as:

$$G = \frac{c_u}{\gamma_u} \frac{c_u}{c_{mob}} = \frac{c_u}{\gamma_u} M \tag{17}$$

representing the shear modulus increasing at higher values of M and correspondingly smaller strains. Now, the average mobilisation factor M in the soil should be of the following form:

$$M \propto \frac{c_u}{\rho gH} \tag{18}$$

governing the "factor of safety" of an undrained excavation. It follows from (17) and (18) that the mobilised soil secant modulus:

$$G \propto \frac{c_u}{\gamma_u} \frac{c_u}{\rho gH} \tag{19}$$

which is recognisable as the first two terms on the right hand side of equation 15. The final term (λ^3/EI) is simply the inverse of wall bending stiffness per unit length, expressed in consistent units. Equation 15 therefore represents the non-

dimensional soil-structure stiffness ratio for soil with a parabolic stress-strain curve up to (c_u, γ_u). The new database can now be used to investigate the relationship between structural response ratio S and soil-structure stiffness ratio R: see Figure 9 where this is shown on log-log axes to capture the enormous range of wall stiffness between sheet-piles and thick diaphragm walls. Very remarkably, the field data fit an exactly inverse relationship (i.e. the slope equals -1.00), with a coefficient of determination of 0.964. This can be written as

$$\log_{10}S = -2.6 - \log_{10}R \qquad (20)$$

and rationalised to give:

$$SR \approx \frac{1}{400} \qquad (21)$$

within an uncertainty factor of 2.9 (calculated as 2 standard deviations) according to Figure 9. The same relationship emerges from the predicted wall displacements using MSD: see Figure 10.

Substituting for S and R from equations 13 and 15 respectively, we can define a normalised displacement factor ψ such that:

$$\psi = SR = \frac{w_{\max}}{\lambda}\frac{1}{\gamma_u}\left(\frac{c_u}{\rho g H}\right)^2 \approx \frac{1}{400} \qquad (22)$$

Notably, the wall bending stiffness has now cancelled out. Figures 9 and 10, together with equations 21 and 22, have shown that wall stiffness has a negligible influence on the amplitude of wall bulging due to excavation. This has been proved for EI ranging within 4 orders of magnitude between sheet-piles and reinforced concrete diaphragms, representing 110 braced retaining walls from around the world.

Equation 22 enables the engineer to estimate maximum wall displacement w_{max} using knowledge only of excavation depth H, clay depth D to a stiff stratum (to calculate λ from equation 14), soil density ρ and shear strength c_u at mid-depth 0.5D, and the reference strain γ_u required for peak strength which can be estimated from plasticity index according to Figure 2. But the possible variation by a factor of up to 2.9 must not be forgotten. This is emphasised in Figure 11 where the normalized displacement factor ψ is plotted on a linear scale against a non-dimensional structural system stiffness η where:

$$\eta = \frac{EI}{\rho_w g \lambda^4} \qquad (23)$$

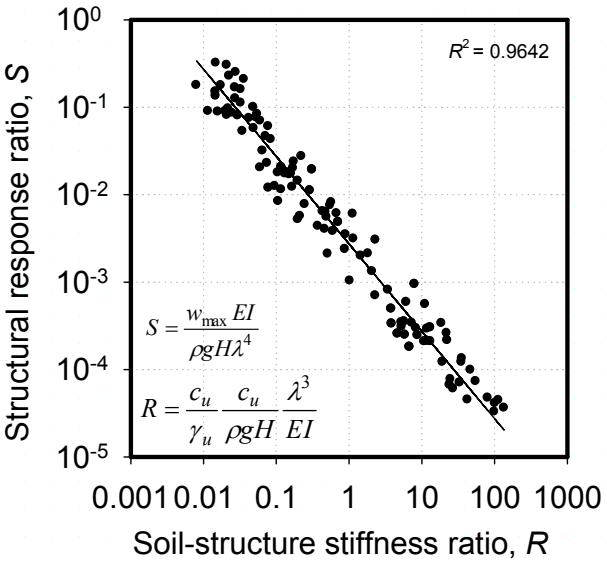

Figure 9 Field data plotted on log S versus log R

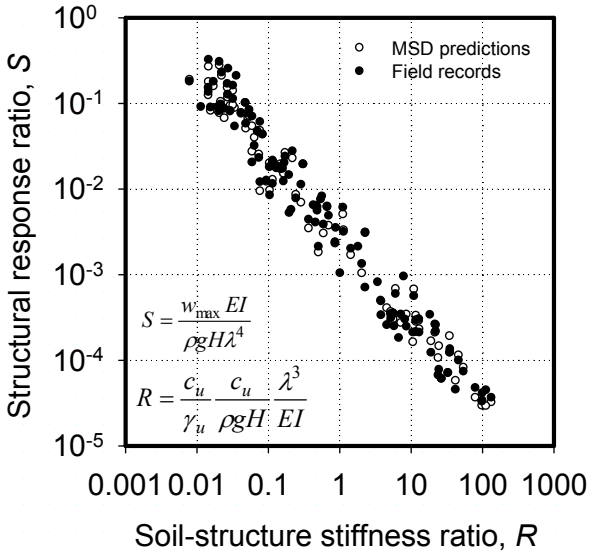

Figure 10 Field data and MSD predictions plotted on log S versus log R

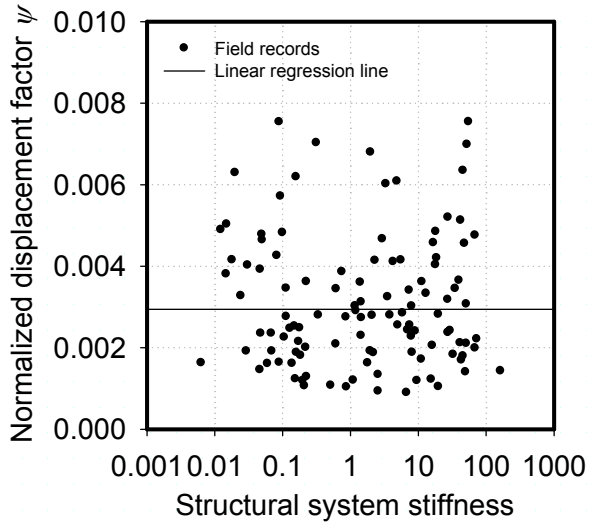

Figure 11 Field data plotted on ψ versus η

The arithmetical average value of ψ for the field data plotted in Figure 11 is 0.003, but the range is about 0.001 to 0.008. It must be recognised that much of this scatter arises from the desire in these charts to represent the excavation construction process in terms of a single mechanism of dimension λ. If the engineer is prepared to take another few hours establishing the possible construction sequence and excavation stages, and performing a cumulative MSD calculation on a spreadsheet, then the scatter of 110 jobs reduces from a factor of about 2.9 (see Figure 9) to a factor of about 1.4 (see Figure 8). Most of this remaining uncertainty is thought to arise from the difficulty of selecting representative values of undrained shear strength c_u and reference strain γ_u. It would be easy to accept that c_u might be uncertain within 10% so that c_u^2 varies within a factor of 1.2. And while the plots in Figures 8 and 9 benefitted from an estimate of γ_u based on the data of site-specific direct simple shear (DSS) tests, shown in Figure 3, the uncertainty factor must again have been about 1.2. A larger uncertainty would have had to be accepted if γ_u had been estimated from plasticity index using Figure 2, of course.

DISCUSSION

It is interesting to use equation 22 to develop an expression for the more familiar term w_{max}/H:

$$\frac{w_{\max}}{H} \approx \frac{\gamma_u}{400}\frac{\lambda}{H}\left(\frac{\rho g H}{c_u}\right)^2 \qquad (24)$$

Normally consolidated clays

Let us now estimate the undrained strength at mid-depth of "soft" clay. Considering normally consolidated high plasticity clay with a high water table:

$$c_u = 0.3\,\sigma'_v = 0.3\,(\rho - \rho_w)\,gD/2 \qquad (25)$$

Taking the corresponding density $\rho \approx 1500$ kg/m^3, and making the necessary substitutions:

$$\frac{w_{\max}}{H} \approx \frac{\gamma_u}{400}\frac{\lambda}{H}\frac{H^2}{D^2}400 \approx \gamma_u\frac{H(D-0.5H)}{D^2}$$

$$\frac{w_{\max}}{H} \approx \gamma_u\frac{H}{D}\left(1-0.5\frac{H}{D}\right) \qquad (26)$$

For example, if $H/D = 2/3$ such that $\lambda = H$, and $\gamma_u = 3\%$, we find:

$$\frac{w_{\max}}{H} \approx 0.44\,\gamma_u \approx 1.3\% \qquad (27)$$

Bolton et al (2008) showed that the average shear strain mobilised in the soil around a bulging wall is

$$\gamma_{average} \approx 2\frac{w_{\max}}{\lambda} \qquad (28)$$

for relatively wide excavations ($B \geq \lambda$), and somewhat larger in the passive zone between the walls for narrow excavations ($B < \lambda$). Combining (24) and (28), we find

$$\gamma_{average} \approx \frac{\gamma_u}{200}\left(\frac{\rho g H}{c_u}\right)^2 \qquad (29)$$

Using the same wall geometry as in (26) and (27) we find that for typical braced excavations in normally consolidated high-plasticity clay:

$$\gamma_{average} \approx \frac{\gamma_u}{200}400\frac{H^2}{D^2} \approx 0.89\,\gamma_u \qquad (30)$$

However, shear strains vary within the assumed deformation mechanism up to a maximum which is $\pi/2$ times the average. And there must ultimately be a tendency to develop a thin slip zone adjacent to the wall. These considerations must lead us to expect first a loss of secant stiffness, and then a drop in strength below the peak, as large deformations develop behind a wall in normally consolidated clay. The rate of wall bulging and ground subsidence would then start to exceed the initial predictions of equation 24, and might result in structural failure. And although the foregoing calculations were predicated on undrained behaviour, the tendency of soil beneath the excavation to swell and soften due to stress relief would compound the problem. It should be considered essential to monitor the wall profile continuously during the excavation of normally consolidated clays.

Overconsolidated clays

If the strength of the clay at its mid-depth was double the normally consolidated value, equation 24 suggests that the wall displacements would correspondingly be reduced by a factor of 4. On the other hand, overconsolidated clays are heavier, and if the bulk density was 25% higher, the wall displacements would be 25% larger. It is not yet clear whether overconsolidation reduces the reference strain γ_u, so this will be regarded as being unchanged. The estimated maximum wall displacement in this "firm" clay, in the same

excavation scenario as that examined for "soft" clay in (25) to (27), would therefore be:

$$\frac{w_{max}}{H} \approx 0.14\,\gamma_u \approx 0.4\% \qquad (31)$$

The useful notion of parabolic stress-strain curves, and the application of dimensional analysis, has allowed us to estimate that wall displacements in firm clays could well be about one third those of the same type of soil, had it been normally consolidated. This offers a straightforward explanation for why it is normally consolidated clays that have caused greatest anxiety, even where braced reinforced concrete diaphragm walls have been used to support the sides.

The retaining wall

These bulging displacements must apparently be regarded as unavoidable, even if a typical diaphragm wall is used. The evidence of Figure 9 suggests that a secant-pile wall or a sheet-pile wall should fare just as well if it were correctly braced or anchored. Measures such as exceptional wall thickness, barrettes or buttresses would be needed to enhance the structural stiffness beyond that of any of the walls in the new database ($R < 0.01$; $\eta > 100$) if bulging was to be suppressed. Only then might the structural strain energy increase to the point where ΔW_{wall} becomes significant compared with ΔW_{soil} in equation 11, and only then might the trend-line of structural response in Figures 9 and 10 curve below the linear regression line established for walls in the existing database. However, the current study does raise the question of whether heavy duty diaphragm walls are necessary or efficient, especially in overconsolidated soils.

An alternative structural design philosophy in stiff clays would be to accept the wall displacements and curvatures implied by equation 24, and to create a well-integrated structure with a wall that was as thin as possible, to minimise bending strains. Of course, other constraints must be met, such as ease of construction, connection to supports, water-tightness and the walls' possible role in vertical load-bearing.

The supports

If the magnitude of bulging displacements estimated in equation 22 pose unacceptable difficulties either for the retaining structure itself or for nearby structures or services, there are relatively few responses that offer a viable remedy. Before considering them, however, it would be wise to establish the situation with greater precision. It should be recalled that equations 22 to 30 derive from the regression in Figure 9 which is subject to an uncertainty factor of 2.9 (at two standard deviations) compared to an uncertainty factor of 1.4 when using incremental MSD. Most of this difference will arise from differences in the bracing regime that are not reflected in the choice of a single representative wavelength λ, as used in equation 22. It follows that by adopting very stringent propping procedures, with close spacing and pre-stressing, an engineer might well be able to reduce the magnitude of bulging by a factor of 2 compared with equation 22. A slack procedure of installing widely-spaced struts could, equally, lead to displacements double those indicated in equation 22. These possibilities could be foreseen by performing appropriate MSD analyses. If further assurance were needed, FEA could be performed using stress-strain data obtained from tests on high quality cores. The risks of adopting inappropriate parameters would then be much reduced if the FE program could accept raw stress-strain data normalised in the fashion of Figure 1, rather than attempting to fit a more general constitutive model. The responsibility for commissioning appropriate stress-strain tests (e.g. DSS tests) on representative high-quality samples would remain with the designer.

If these more rigorous calculation procedures fail to assure the designer that structural damage could be avoided using a conventional wall with high quality bracing, then additional methods of support will have to be considered. Some of them are considered below.

As mentioned earlier, the excavation could be carried out under water. Archimedes principle could be invoked, with the bulk density ρ in equation 22 being replaced by $(\rho - \rho_w)$, which may be only one third of its previous value. When squared, as indicated, this would offer a reduction factor of 9 in the maximum wall displacement.

Another possibility is to pre-construct deep in situ props between the walls, prior to excavation. Access shafts could be sunk at intervals between the walls to enable precast concrete props to be installed in sections by jacking. In situ props could be designed to limit wall bulging to any required extent. Something similar can be achieved by introducing zones of jet grouting, deep mixing, or some other method of ground improvement, to prop apart in situ walls once they have been introduced to their full depth: Shirlaw et al (2006). However, it would be dangerous to place such props in the expectation of easily removing them again during the excavation process. If they were effective as props during the excavation process, they will have developed strong compressive reactions. Extremely stringent conditions would need to be set for the casting of their permanent replacements prior to their removal, therefore.

One example of a permanent "prop" created by ground improvement is a base plug or slab of stabilized soil introduced by jet grouting or deep mixing, placed between the side walls, and just above their base. Plugs have the ability to prevent wall base translation, thereby converting a "floating" wall (Figure 4c) into a fixed-base wall (Figure 4d). This will have the effect of reducing both the amplitude of wall displacement w_{max}, and its lateral extent λ. Such plugs are generally more than 2 m deep to ensure that soft spots due to poor mixing do not compromise the integrity of the support system. Particular care has to be taken to avoid soft clay remaining at the interface between the wall and the plug, since that would compromise both the axial stiffness of the plug as a prop and its shear resistance, which is required to resist soil and water pressures from below when the excavation has been completed.

From the standpoint of construction efficiency and cost, the question often arises of the optimization of temporary propping within the excavation. There are some significant difficulties.

- The pre-existing earth pressures will be difficult to assess. Only normally consolidated soils will have earth pressure coefficient $K_{o,nc} \approx 1 - \sin\phi$; overconsolidated soils will possess a higher value.
- The construction of a cast-in-situ wall alters the earth pressure, bringing it close to the pressure of wet concrete (but not exactly, due to 3D construction effects): Richards et al (2006).
- The first stage of excavation, prior to the fixing of any struts or anchors, induces cantilever rotation or bending (Figures 4a, 4b) which mobilises some soil strength, c_{mob} or ϕ_{mob}, depending on the permitted strains. Whilst doing so, the major principal stress remains nearly vertical, so that lateral pressures outside the excavation drop to mobilised active values, in which c_{mob} replaces c_u in equation (1) for example: Bolton and Powrie (1988).
- The subsequent placement of props, with excavation taking place below, leads to wall bulging and the further mobilisation of soil strength, but no longer in a simple "active" condition. The shearing in the upper region of soil behind the props will be on vertical planes, so the prop forces have no reason to reduce. Indeed, as the earth pressure behind the deeper, unpropped portion of the wall reduces, overall horizontal equilibrium may require that propping forces in the upper portions increase.
- On the other hand, various factors such as non-rigidity of props, delays in their installation, or the introduction of gaps on purpose, can lead to a further phase of outward wall movement at the top, with stress relaxation leading to smaller prop forces.
- Temperature changes after installation can lead to significant changes in prop force, and to both cyclic and permanent wall movements: e.g. Batten and Powrie (2000).
- Continuity and ductility of props and their connections is very important, but difficult to assure because of the tendency for plastic buckling: Williams and Waite (1993).
- The accidental failure or purposeful removal of a prop or props must lead to load redistribution, and can engender progressive collapse unless sufficient redundancy has been designed-in:.Gaba et al (2003).

In these circumstances it is understandable that designers generally resort to recommendations for prop load distributions based on empirical observations: Terzaghi and Peck (1948), Twine and Roscoe (1999). Optimization must be seen in the context of monitoring construction and design-as-you-go.

Limits on w_{max}/λ

Equation 22 (rewritten as equation 24) sets an average expectation for the bulging w_{max} of a braced wall in terms of the average deformation wavelength $\lambda = D - 0.5H$ down to its fixed base at depth D, during the creation of an excavation of depth H within a soft to firm clay stratum. The key parameters are the mid-depth undrained shear strength c_u and the shear strain γ_u required to mobilise it. This estimate can be refined for greater accuracy by using MSD incrementally with actual (intended) prop spacings and excavation phases, together with the actual soil strength profile.

The acceptability of the w_{max} value in any particular application depends on three criteria:

1. the avoidance of serious damage within the retaining wall itself;
2. the avoidance of serious damage within pre-existing structures or services nearby;
3. the ability to control the safety of the construction process by monitoring deformations and introducing additional supports if necessary.

Regarding the first criterion, it is easily shown that the maximum tensile strain at a sinusoidal bulge of magnitude w_{max} and wavelength λ in a wall of thickness d is given by:

$$\varepsilon_{\max} = \pi^2 \frac{w_{\max} d}{\lambda^2} \qquad (32)$$

In the case of a 0.8 m thick diaphragm wall bulging 0.2 m over an average 20 m wavelength, for example, (31) gives $\varepsilon_{max} \approx 2 \times 10^{-3}$ assuming that the neutral axis of bending remains roughly central. Tensile cracking begins in concrete at $\varepsilon_{crack} \approx 10^{-4}$, longitudinal steel reinforcement yields at about $\varepsilon_{yield} \approx 1.5 \times 10^{-3}$ and concrete crushing typically begins in compression at $\varepsilon_{crush} \approx 4 \times 10^{-3}$: Park and Gamble (2000). So the structural designer may, with care, be able to design the wall as an under-reinforced, fully cracked section which maintains ductility at its ultimate moment of resistance as the wall bulges. A thorough incremental analysis with MSD would provide a more realistic wall profile from which a better estimate of curvature could be made. But it is argued here that it is the continuity of the wall that is paramount during excavation, recalling that equation 22, derived from the case studies, demonstrated the inconsequentiality of wall flexural stiffness to its own deflected profile. The role of the wall is to span between close-spaced props and to prevent local shear failure beneath the props.

Burland and Wroth (1974) showed that the potential damage to structures with shallow foundations can best be assessed in relation to the relative settlement Δ/L, defined as the maximum offset Δ from an initial chord length L. This can be equated here to w_{max}/λ. Burland et al (2001) explain in detail how to apply this concept to the assessment of damage accompanying tunnelling settlement. It is sufficient here to note that the maximum tensile strain induced in a building is roughly equal to $1.3\Delta/L$, and that severe damage is likely to occur beyond a tensile strain of 0.3%. Accordingly, a subsidence trough with relative settlement $w_{max}/\lambda > 0.2\%$ is likely to cause severe damage. It is instructive to compare this with the estimate made in equation 30 for the bulging of a typical wall supporting an excavation in firm clay, $w_{max}/\lambda \approx 0.14\gamma_u$. This could be no more than 0.14% in a low plasticity clay, or as high as 0.7% in a high-plasticity clay, as indicated in Figure 3. It will often be necessary to demolish and rebuild buildings adjacent to deep excavations in soft to firm clay, unless measures (additional to conventional bracing) are used to suppress bulging. Because the whole depth D of clay is initially involved in the cantilever phase of wall movement prior to placing any props, see Figure 4a, structures and services within a distance D from the wall must be regarded as most vulnerable, and meriting detailed analysis.

The third criterion which may place a limit on wall displacements is the controllability of the excavation process through monitoring. Uncertainty over the selection of a representative value for c_u from ground information prior to construction is compounded by the influence of localisation, softening and creep during construction – all of which are exacerbated as peak strength is approached. This suggests the desirability of providing a margin of safety (or a mobilisation factor M) of at least 1.2 against the best estimate of undrained peak strength. Assuming a parabolic undrained mobilisation curve, equation 4b, this corresponds to a restriction $\gamma \leq 0.69\gamma_u$. Equation 28 translates this into a suggested restriction on maximum wall movement:

$$\frac{w_{max}}{\lambda} \leq 0.35\gamma_u \qquad (33)$$

Whereas this might permit $w_{max}/\lambda \leq 1.4\%$ in a compliant plastic clay such as Singapore Marine Clay which has $\gamma_u \approx 4\%$, it would set a stricter limit of $w_{max}/\lambda \leq 0.4\%$ in Boston Blue Clay with $\gamma_u \approx 1\%$, referring to Figure 3.

Equation 33 represents an attempt to ensure that the rate of displacement with ongoing excavation remains manageable. Construction monitoring, which should be regarded as essential, should then be able to keep pace with events and permit sufficient time to recognise the approach of failure so that additional support can be provided.

CONCLUSIONS

1. A new database of clay stiffness has been used to demonstrate that the undrained stress-strain curve of soft to firm clays can be regarded for practical purposes as a parabola with its apex at the origin, passing through the point (c_u, γ_u) where γ_u is found to be related to plasticity index.

2. An incremental Mobilizable Strength Design method for deep excavations has been formulated in which conservation of energy is applied stage by stage to a repertoire of assumed deformation mechanisms. Deformations are accumulated, but account is taken of soil non-linearity. MSD predictions were compared with the results of Finite Element Analysis previously carried out by Jen (1998); discrepancies are smaller than 30%.

3. A new database of 155 field case studies of excavations in soft to firm clays has been compiled from 9 cities worldwide. Of these, 110 studies are sufficiently detailed to permit MSD back analyses for comparison with actual measurements of maximum wall displacement. It is shown that 90% of MSD predictions fall within a factor of 1.4 of the actual measurements.

4. New dimensionless groups have been defined using concepts arising from MSD analysis. These are based on the typical deformation mechanism, taken to be that applying when the excavation is 50% constructed. A soil-structure stiffness ratio *R* accounts for parabolic non-linearity of the soil. A new structural response ratio *S* normalises the lateral pressure required to create a given wall bulge by dividing it by the total vertical earth pressure removed in the excavation. Both *R* and *S* involve the flexural stiffness of the wall, *EI*.

5. When $\log_{10}S$ was plotted against $\log_{10}R$ for the field data, the linear regression had a slope of -1, with a high coefficient of determination ($R^2 = 0.964$). This indicates an inverse relationship, proving that *RS* is a constant, and that *EI* cancels out. A new normalised displacement factor ψ = RS is defined with regression offering a value of 1/400. This permits deformations to be predicted within a factor of 2.9. The additional influence of staged construction and prop spacing is inherent to MSD, explaining its better performance within a factor of 1.4. One striking outcome is the proven irrelevance of wall stiffness within the range from sheet-piles to diaphragm walls. The wall projecting below the bottom level of props behaves as flexible in relation to the adjacent soil, at least in the 110 cases that have been examined.

6. Relative wall deformation w_{max}/H is proportional to the reference strain γ_u, inversely proportional to the square of the stability number, and is also influenced by prop spacing ratio in a manner that has not yet been included in a simple formula. It has been demonstrated that large deformations must be expected of braced walls in normally consolidated clays, bringing the soil close to failure. Stiffening the wall sufficiently to reduce deformation is unlikely to be economic. The use of soil stabilisation technology, to construct deep in situ “props” prior to excavation, is more promising.

7. The design of props is best undertaken with respect to existing rules based on previous observations. Optimization is best understood in relation to construction monitoring and design-as-you-go.

8. Excavations, especially in soft clays, are risky. They should be monitored carefully during construction. Setting a limit for the ratio w_{max}/H observed during construction may be rational in relation to three issues: the avoidance of serious damage to the retaining wall itself; the avoidance of serious damage to pre-existing structures or services nearby; the ability to control the rate of deformation by preventing soil from approaching too close to its mobilization of peak strength. Rational limiting values are suggested in relation to the particular characteristics of the job. This makes it difficult to regulate in terms of simple fixed limits, although procedures are recommended for engineers to follow.

9. It has been demonstrated that deep excavations in soft clay pose an unusual deformation problem. In the past, engineers have relied on measuring soil strength and using conventional safety factors. It has now been demonstrated that the acquisition of soil stress-strain data is essential to predicting field behaviour. Simple formulae then predict deformations within a factor of 2.9 (two standard deviations) within minutes. MSD, in a few hours on a spreadsheet, can make more accurate predictions of the staged deformation profile, both wall displacements and subsidence trough, within a factor of 1.4. It is unclear in simple cases whether FEA would offer better predictions that that: ground parameters especially remain inherently difficult to assess. However, FEA using a simple parabolic stress-strain relation for clays, might be very valuable for analysing unusual designs.

10. There is a need for further work on mechanisms associated with volume change, such as for clay consolidation or for sands.

REFERENCES

Anderson, D. G. and Richart, F.E. (1976) Effect of straining on shear modulus of clays. Journal of the Geotechnical Engineering Division ASCE, Vol. 102, No. GT9, pp. 975-987.

Batten M. and Powrie W. (2000) Comparison of measured and calculated temporary prop loads at Canada Water station, Geotechnique, Vol. 50, No. 2, pp. 127-140.

Bjerrum, L., and Landva, A. (1966) Direct simple-shear test on a Norwegian quick clay. Geotechnique, 16, No.1, 1–22.

Bolton, M.D., Lam, S.Y. and Osman, A.S. (2008) Supporting excavations in clay - from analysis to decision-making. 6th International Symp. on Geotechnical Aspects of Underground Construction in Soft Ground, Taylor and Francis, pp. 15-28.

Bolton, M.D. and Powrie, W. (1988) Behaviour of diaphragm walls in clay prior to collapse, Geotechnique, Vol. 38, No.2, pp. 167-189.

Boone S.J. (2006) Deep Excavations: General Report. 5th International Symp. on Geotechnical Aspects of Underground Construction in Soft Ground, Amsterdam, pp. 23-31.

British Standards Institution (1994). Code of practice for earth retaining structures. BS 8002.

Burland, J.B. and Wroth, C.P. (1974) Settlement of buildings and associated damage. Proceedings of Conference on Settlement of Structures, Cambridge, Pentech Press, pp. 611-654.

Burland, J.B., Broms, B.B. and de Mello, V.H.B. (1977) Behaviour of foundations and structures. Proceedings of 9th International Conference on Soil Mechanics and Foundation Engineering, Tokyo, Vol. 2, pp. 495-546.

Burland J.B., Standing J.R and Jardine F.M. (2001) Building Response to Tunnelling: Case Studies from Construction of the Jubilee Line Extension, CIRIA Special Publication 200, Thomas Telford.

Clarke P.J. and Prebaharan, N. (1987) Marina Bay Station, Singapore, excavation in soft clay, Proceedings of Case Histories in Soft Clay, NTU, Singapore, pp.95-107.

Diaz-Rodriguez, J.A., Leroueil, S. and Aleman, J.D. (1992).Yielding of Mexico City clay and other natural clay. Journal Geotechnical Div. ASCE, Vol.118, No.7, July, 1992.

Finno, R.J. and Chung, C.K. (1990). Stress strain strength responses of compressible Chicago Glacial clays. Journal Geotechnical Division ASCE, Vol.118, No.10, pp. 1607-1625.

Gaba A.R., Simpson B., Powrie W. and Beadman D.R. (2003) Embedded retaining walls – guidance for economic design, CIRIA Report C580, CIRIA, London.

Hunt, C. E., Pestana, J. M., Bray, J. D., and Riemer, M. (2002). Effect of pile driving on static and dynamic properties of soft clay. Journal Geotechnical and Geoenvironmental Engineering, Vol.128, No.1, pp.13–24.

Jen, L.C. (1998). The design and performance of deep excava-tions in clay. PhD thesis, Dept. of Civil and Environmental Engineering, MIT.

Kim, T. C. and Novak, M. (1981) Dynamic properties of some cohesive soils of Ontario. Canadian Geotechnical Journal, Vol. 18, pp. 371-389.

Lam (2010) Ground movements due to deep excavation: physical and analytical models. PhD thesis, University of Cambridge.

Lam, S.Y. and Bolton, M.D. (2010) Energy conservation as a principle underlying mobilizable strength design for deep excavations, ASCE Journal of Geotechnical and Geoenvironmental Engineering, to be published.

Lin, H.D. and Wang, C.C. (1998). Stress strain time function of clay. Journal Geotechnical and Geoenvironmental Engineering, ASCE, Vol. 124, No. 4, pp. 289-296.

Magnus, R., The, C.I. and Lau, J.M. (2005) Report of the Committee of Inquiry into the incident at the MRT Circle Line worksite that led to the collapse of Nicoll Highway on 20 April 2005, Singapore Government Ministry of Manpower.

Moh, Z.C., Nelson, J.D. and Brand, E.W. (1969). Strength and Deformation behaviour of Bangkok clay. ICSMFE VII, Mexico, 1969, pp.287-295.

O'Rourke, T.D. (1993) Base stability and ground movement prediction for excavations in soft clay. Retaining Structures, Thomas Telford, London, pp. 131-139.

Osman, A.S. and Bolton, M.D. (2004) A new design method for retaining walls in clay. Canadian Geotechnical Journal, 41 (3), 451-466.

Osman, A.S. and Bolton, M.D. (2006) Ground movement predictions for braced excavations in undrained clay. ASCE Journal of Geotechnical and Geo-environmental Engineering, 132 (4), 465-477.

Park R. and Gamble W.L. (2000) Reinforced Concrete Slabs, John Wiley & Sons.

Richards, D.J. , Clark, J. and Powrie, W. (2006) Installation effects of a bored pile wall in overconsolidated clay, Geotechnique Volume 56, No. 6, pp. 411-425.

Shibuya, S. & Mitachi, T. (1994) Small strain modulus of clay sedimentation in a state of normal consolidation. Soils and Foundations, Vol. 34, No.4, pp. 67-77.

Shirlaw, J.N., Tan T.S. and Wong, K.S. (2006) Deep excavations in Singapore Marine Clay. 5th International Symposium on Geotechnical Aspects of Underground Construction in Soft Ground, Amsterdam, pp. 1-16.

Stroud, M. A. (1974) The Standard Penetration test in sensitive clays and soft rocks. Proc. European seminar on penetration testing, Stockholm, Vol. 2:2, pp. 366-375.

Tan, T.S. and Shirlaw, J.N. (2000) Braced excavation – Excavation in general, 3rd International Symposium on Geotechnical Aspects of Underground Construction in Soft Ground, Tokyo, pp. 53-62.

Twine D. and Roscoe H. (1999) Temporary propping of deep excavations – guidance on design, CIRIA Report C517.

Vardanega, P.J. and Bolton, M.D. (2010) The stiffness of clays and silts, under review.

Vucetic M. and Tabata K. (2003) Influence of soil type on the effect of strain rate on small-strain cyclic shear modulus. Soils and Foundations, Vol. 43, No.5, pp.161-173.

Whittle, A.J. (1993). Evaluation of a constitutive model for overconsolidated clays. Geotechnique, 43, No.2, pp. 289-313.

Williams B.P. and Waite D. (1993) The design and construction of sheet piled cofferdams, Special Publication 95, CIRIA, London

Wong, K. S., Broms, B. B. (1989). Lateral wall deflections of braced excavations in clay. ASCE Journal of Geotechnical Engineering, Vol. 115, No. 6, pp. 853-870.